Electronic Supplementary Information

Biocompatible pH-responsive nanoparticles with a core-anchored multilayer shell of triblock copolymers for enhanced cancer therapy

Elizabeth Ellis,[a,b,c] Kangyi Zhang,[c] Qianyu Lin,[d] Enyi Ye,[c] Alessandro Poma,[a] Giuseppe Battaglia,[a,e] Xian Jun Loh,[c,d] and Tung-Chun Lee[*a,b]

[a.] Department of Chemistry, University College London (UCL), United Kingdom
[b.] Institute for Materials Discovery, University College London (UCL), United Kingdom. E-mail: tungchun.lee@ucl.ac.uk
[c.] Institute for Materials Research and Engineering (IMRE), Agency for Science Technology and Research (A*STAR), Singapore
[d.] Department of Materials Science and Engineering, National University of Singapore, Singapore
[e.] Department of Chemical Engineering, University College London (UCL), United Kingdom

1. Experimental

1.1. Materials and methods

Oligoethylene glycol methl ether methacrylate (OEGMA) average M_n = 500 g / mol, diisopropylamino ethyl methacrylate (DPA), bis[2-(2'-bromoisobutyryloxy)ethyl]disulfide, copper bromide (CuBr) (99.99%), 2,2-Bipyridyl (BiPy), tris(2-carboxyethyl)phosphine hydrochloride (TCEP), methanol, ethanol and dichloromethane were ordered from Sigma Aldrich, UK and used without further purification. DI H_2O was Milli-Q water with a resistivity of 18.2 MΩ·cm. 2-(Methacryloyloxy)ethyl phosphorylcholine monomer (MPC, 99.9% purity) was donated by Biocompatibles U.K. Ltd. $HAuCl_4$ 99.999% (Alfa Aesar), sodium citrate (Sigma Aldrich), phosphate buffered saline (PBS) (Gibco Life Technologies), heat inactivated fetal bovine serum (FBS) (Gibco), phosphotungstic acid (PTA), doxorubicin HCl (International Laboratories 99%), were ordered from Singapore and used without further purification.

NMR measurements were carried out on a Bruker Avance III 600 MHz or 400 Mhz spectrometer. GPC was performed on a GPCMax equipped with an RI detector from Malvern Technologies (Greater Malvern, UK) with acidic water (0.25 vol% TFA in water) as solvent on a Novamax column (including guard column) from PSS Polymers (Mainz, Germany). DLS was performed on a Malvern Zetasizer Nano ZS. TEM was performed on a FEI Titan Transmission Electron Microscope. Grids of carbon-coated copper mesh were prepared by spotting and drying of solutions 3 times. For stained samples, solutions were spotted and dried, then placed in 0.75 % PTA stain solution for 2 seconds and dried again. UV-vis was performed on a Shimadzu UV-2501 PC. Fluorescence was performed on a Shimadzu RF-5301 PC.

1.2. Preparation of thiolated POEGMA-PDPA-PMPC

Oligoethylene glycol methl ether methacrylate (OEGMA) (1.38 mL, 3 mmol) bis[2-(2'-bromo-isobutyryloxy)ethyl]disulfide (8.3 μL, 0.027 mmol) were added to 1.5 mL methanol in a round bottom flask. After degassing (45 mins N_2) CuBr (15 mg) and BiPy (35 mg) were added. Once conversion was complete (100% from ^{1}H NMR integrals), degassed diisopropylamino ethyl methacrylate (DPA) (0.96 mL,

4.05 mmol) and ethanol (1 mL) were injected into the mixture. Once conversion of DPA was sufficient, degassed MPC (0.965 g, 3.27 mmol) and ethanol were injected. Upon completion, the reaction was stopped by exposure to air and addition of ethanol. The product was passed through a silica column and dialysed against DCM x2, MeOH x2 and DI water x2 and freeze dried. If GPC showed remaining uncleaved disulphide, reduction was carried out in DI H_2O at a polymer concentration of 1 mg mL^{-1} with 1 molar eqv. TCEP for 30 mins under N_2, then dialysed against EtOH and H_2O and freeze dried.

1.3. ^{1}H nuclear magnetic resonance (NMR) of POEGMA-PDPA-PMPC triblock copolymer

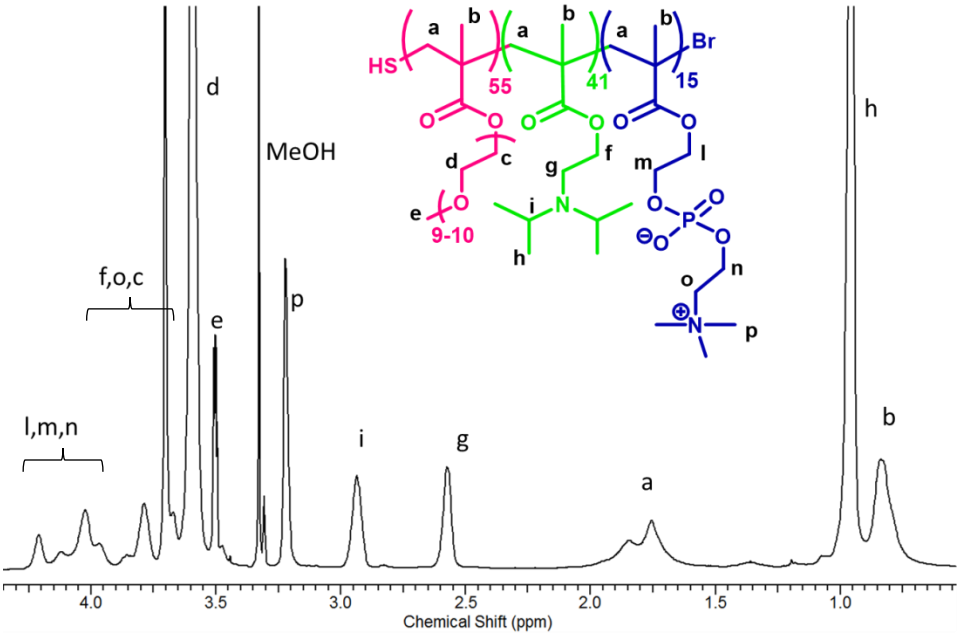

Fig. S1. ^{1}H NMR spectrum of HS-POEGMA-PDPA-PMPC in MeOD/$CDCl_3$.

1.4. Gel permeation chromatography (GPC) of POEGMA-PDPA-PMPC triblock copolymer

GPC elution vol: 7.8, M_w: 186374 PDI: 1.55 (based on PEG standard). The relatively high polydispersity could be due to a number of factors, including the coordination of DPA to the copper(I) catalyst in place of the intended ATRP-ligand and the low solubility of the PDPA in the solvent system.[1, 2] It is not unusual to see similar systems with a polydispersity of 1.4.[3, 4]

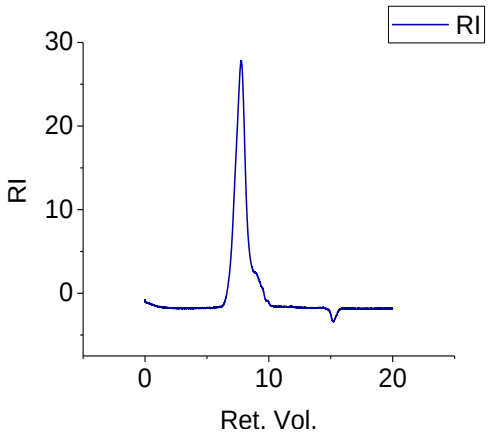

Fig. S2. GPC trace of HS-POEGMA-PDPA-PMPC.

1.5. Gold nanoparticle (Au NP) synthesis

Gold nanoparticles were prepared following literature procedure.[5] Briefly 150 mL sodium citrate solution (2.2 mM) was heated under reflux to 100 °C. $HAuCl_4$ solution (1 mL, 25 mM) was injected and the solution rapidly changed from yellow to purple then to red. After 30 mins, sodium citrate (1 mL, 60 mM) and $HAuCl_4$ (1 mL, 25 mM) were sequentially injected. This was repeated after a further 30 mins. Nanoparticles were characterised by DLS and TEM. D_h = 24.7 nm; $size_{TEM}$ = 15.5 ± 2.5 nm; concentration of Au NPs = ~2.62 x 10^{12} NPs/mL.

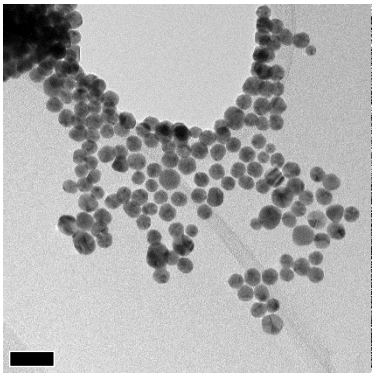

Fig. S3. TEM image of citrate-coated gold nanoparticles. Scale bar = 50 nm.

1.6. Polymer coating of gold nanoparticles

Polymer solution (3 mL, 1 mg mL^{-1}) was prepared in DI H_2O at pH 2. 3 mL of Au NP solution was added gradually over 15 min. After 30-min stirring, 1.5 mL of 3M NaCl was added. After stirring overnight, the solution was centrifuged (10 krpm, 30 min) and redispersed in dilute HCl (10 mM, pH 2).

In order to confirm the purity of the construct with regards to whether there is any remaining polymer that has not been removed by centrifuge, DLS measurement was performed before and after purification by centrifuge (Fig. S4). It can be seen when looking at intensity by volume that there is residual polymer before centrifuging which appears as peaks at low hydrodynamic diameter (d < 10 nm), corresponding to nanoscale aggregates (e.g. micelles) of the free polymer. After redispersal these peaks are no longer present.

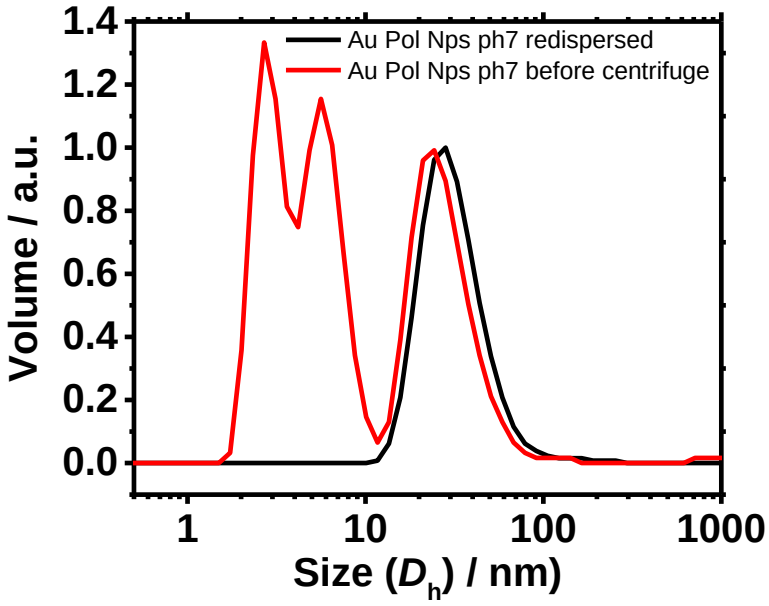

Fig. S4. DLS of polymer-coated gold nanoparticles before (red) and after (black) centrifugation to remove excess polymer.

The grafting density is estimated to be ~0.11 chains / nm^2 (i.e. polymer footprint ~8.8 nm^2 and ~86 chains / NP). This is calculated based on the average diameter of Au NPs (15.5 ± 2.5 nm) and the dried polymer shell thickness (4.0 ± 0.9 nm) determined by TEM (Fig. 2d), average molecular weight of the polymer (40.7 kDa) determined by ^{1}H NMR, and by assuming the average density of the polymer shell to be 1.2 g / mL. Briefly, for a nanocarrier, the volume of the polymer coating is given by the difference between the total volume of the nanocarrier (dry state) and that of the Au NP core. Mass of the coating will then be estimated based on the density. The total number of chains per nanocarrier will be given by dividing the mass by the MW of the polymer multiplied by Avogadro's Constant. Finally the grafting density will be calculated by dividing the number of chains by the surface area of the Au NP core. The resultant grafting density is consistent with the theoretical, fully extended length of the OEGMA chains (3.6 nm), verifying the proposed compact inner shell structure.

2. Colloidal stability of polymer-coated Au NPs in PBS and FBS

Polymer-coated nanoparticles and citrate-coated nanoparticles were redispersed in DI H_2O. DLS and UV-vis measurements were then taken at pH 2 and pH 7. Samples at pH 7 were added to PBS and FBS (1:1 by volume), then DLS and UV-vis were measured at time intervals.

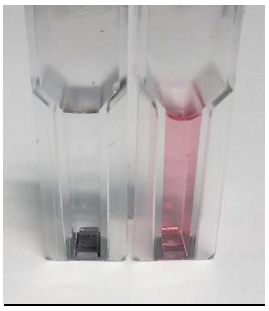

Fig. S5. Photograph of citrate-coated Au NPs (left) and polymer-coated Au NPs (right) in 50% PBS.

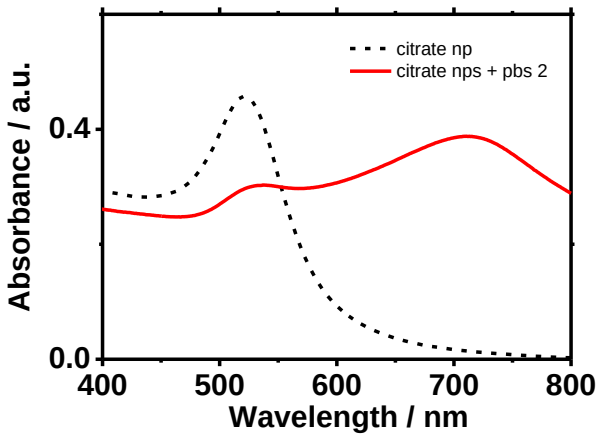

Fig. S6. UV-vis of citrate-coated Au NPs in water (black dash) and PBS (red).

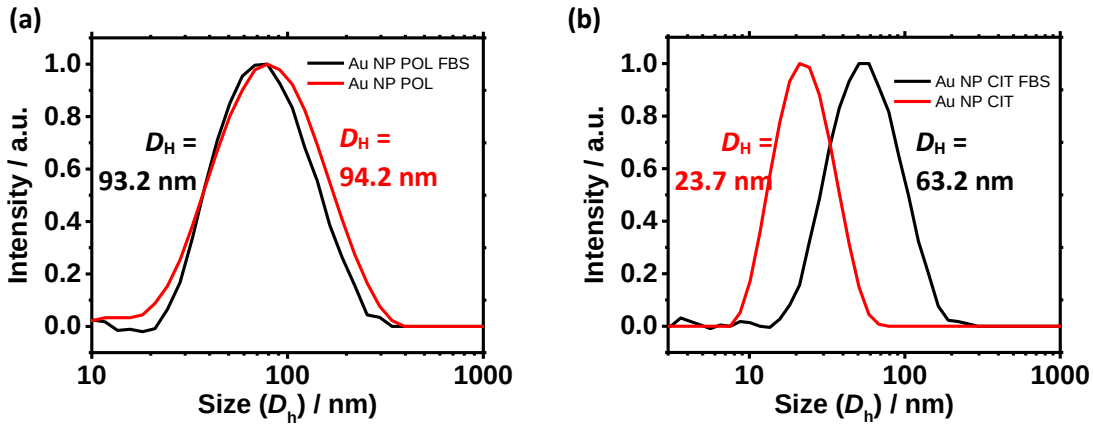

Fig. S7. Antifouling of nanocarriers. DLS size distribution of (a) polymer-coated and (b) citrate-coated Au NPs in water (pH ~7) and in 50% FBS. The background of the FBS curves has been corrected by subtracting the proportionated DLS size distribution curve of pure FBS which shows a single peak at ~8 nm. Reported D_H is estimated based on weighted average (= $(\sum^n xi \cdot yi)/(\sum^n yi)$) of the peak.

3. POEGMA-PDPA-PMPC block lengths and shell thickness on Au NPs

Table S1. Theoretical maximum extended chain lengths of polymer blocks.

Block	DP_n (^{1}H NMR)	Theoretical maximum length / nm[a]
POEGMA	55	13.8
PDPA	41	10.3
PMPC	15	3.8
Overall	111	27.9

Table S2. Polymer shell thickness on Au NPs

	Theoretical maximum[a]	Actual hydrated (DLS)[b]	Actual dried (TEM)[c]	Change with pH (DLS)[d]
Shell thickness / nm	27.9	23.0	4.0 ± 0.9	3.4

[a] Theoretical maximum length of a block is calculated based on the number of repeating units which is estimated by the degree of polymerisation from the integration of the peaks in the ^{1}H NMR spectra.

[b] This is obtained by 0.5 x ($D_{h,\ polymer\text{-}Au\ NPs} - D_{h,\ Au\ NPs}$), see Fig. 2c.

[c] This is estimated by measuring the thickness of the bright halo of the PTA-stained polymer-Au NP sample.

[d] This is estimated by 0.5 x ($D_{h,\ polymer\text{-}Au\ NPs,pH2} - D_{h,\ polymer\text{-}Au\ NPs,pH7}$), see Fig. 3b.

The ratio between the theoretical length and the observed shell thickness can be used as a measure of the degree of coiling and packing of the polymer within the shell. This ratio for POEGMA-PDPA-PMPC triblock copolymer anchored on an Au NP is approximated to be 27.9 / 23.0 = 1.2. This is consistent with those reported by Muller *et al.*[6, 7] In line with our train of thoughts, the ratio of the POEGMA-PDPA-PMPC is at the lower end of the range because of the bulky side chains on the POEGMA and PMPC, reducing the coiling of the polymer by steric hindrance. As a result, the POEGMA-PDPA-PMPC adopts a more linear conformation which is favourable to the formation of a well-defined multilayer shell around the Au NP.

4. Preparation and characterisation of DOX-loaded nanoparticles

To encapsulate the drug within the hydrophobic PDPA block of the polymer coating, 25 wt % DOX•HCl with respect to the amount of polymer was incorporated into the initial pH 2.3 aqueous solution of the polymer before addition of any nanoparticles. Once the polymer coating was complete, the pH of the solution was increased to pH 7.2 to trap the DOX within the hydrophobic part of the polymer. Excess DOX and polymer were then removed by a centrifugation-redispersion cycle. The amount of DOX encapsulated was calculated by measuring the remaining DOX in the supernatant of the encapsulation solution after removal of the DOX-loaded nanoparticles. Because of the high concentration of DOX in the supernatant, the solution had to be significantly diluted before fluorescence could be quantified. It is noted that this step could introduce uncertainty in fluorescence measurement and hence in the amount of encapsulated DOX. Fluorescence measurements show that

the concentration of DOX in the supernatant after centrifugation decreased by 40.6 µg/mL, implying that this amount has been encapsulated by the nanocarriers. The encapsulation efficiency (defined as '(amount of DOX encapsulated / amount of DOX added) x 100 %') was calculated as 0.0406 mg mL^{-1} / 0.11 mg mL^{-1} x 100 % = 37 %.

5. Doxorubicin release studies

3 vials of 3 mL of DOX-loaded nanoparticles were prepared. DOX-loaded nanoparticles were incubated at 37 °C in the dark at pH 7.2. DOX release was monitored by collecting 300 µL of solution, centrifuging out the nanoparticles, measuring the fluorescence of the supernatant and quantifying the concentration by comparison with the calibration curves. After 24 hours, the pH of the nanoparticle solutions was decreased to ~4.0 by addition of HCl to each solution. The solutions were monitored periodically for DOX concentration. DOX fluorescence at t = 0 was attributed to unencapsulated DOX and subtracted from the time points as background.

In order to verify that DOX is stable to purification by centrifugation at pH 7, a blank has been performed. Briefly, a solution of DOX (40.6 µg mL^{-1}) was prepared in buffer at pH 4.3, the pH was increased to 7.2 and the concentration of DOX was determined by fluorescence spectroscopy before and after centrifuging (10,000 rpm, 20 min). It was found that the concentration of DOX decreased by 0.44 µg mL^{-1} following centrifugation. This is an insignificant amount (within error bars) and would not have an effect on the data presented.

6. Cell studies

6.1. Cell viability study Au-NP without DOX

Cell viability assay was done using resazurin assay (CellTiter-Blue® Promega) to determine if the nanoparticle vehicle is cytotoxic. NIH/3T3 fibroblasts (ATCC® CRL-1658™) were cultivated according to ATCC® protocols. Cells were seeded onto 96 well plates at 1 x 10^5 cells/ml (100 µL per well). 24 hours after seeding, we added 100 µL of nanoparticles (concentration = ~1.05 x 10^{12} NPs/mL) to incubate for 24 h or 48 h. Fluorescence reading was taken using Tecan Infinite M200 plate reader.

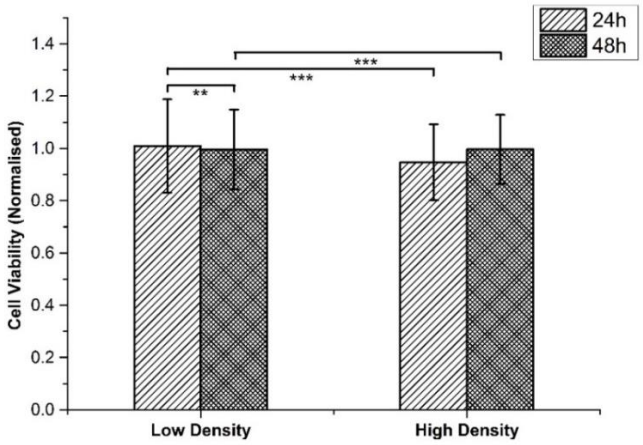

Fig. S8. Cell viability of NIH/3T3 fibroblasts of varying cell density treated with nanoparticles for 24h and 48h. Fluorescence readings from resazurin assay were normalised with respective control data. The nanoparticles are non-toxic as seen from the high cell viability. (Low cell density = 5 x 10^4 cells / mL. High cell density = 2 x 10^5 cells / mL. **p<0.01, ***p<0.001)

6.2. Cell viability after treatment with NP-DOX and DOX (Fig 4b)

MCF-7 (ATCC® HTB-22™) breast adenocarcinoma cells were cultivated according to ATCC® protocols. Efficacy of NP-DOX and DOX was determined using resazurin assay as before. Cells in culture flasks were seeded onto 96-well microplates at densities of 1 × 10^4 cells per well. 24 hrs after cell seeding, media containing either NP-DOX (concentration = ~1.05 x 10^{12} NPs/mL) or DOX (50 µg mL^{-1} which is equivalent to the estimation of the amount of encapsulated DOX for this experiment) was added to the respective wells. The control treatment is media without any additive. The experiments were done in replicates of six and the incubation time was 24 hrs. Fluorescence was quantified using TECAN Infinite® M200 at excitation/emission wavelengths of 560nm/590nm.

6.3. Fluorescent microscopy for doxorubicin uptake (Fig 4 c-d)

MCF-7 (ATCC® HTB-22™) breast cancer cells were cultivated based on ATCC protocols. Cells in culture flasks were seeded onto 24-well microplates at a density of 50,000 cells per well. NP-DOX (concentration = ~1.05 x 10^{12} NPs/mL) or DOX (61 µg mL^{-1} which is equivalent to the estimation of the amount of encapsulated DOX for this experiment) was added to the respective wells. After 1-hour incubation, samples were fixed with 4% glutaraldehyde then washed with PBS. Cells were then permeabilised in 0.1% Triton X-100 before staining in DAPI solution. This was followed by mounting in ProLong Gold antifade reagent (Thermo Fisher Scientific) and visualization using a Leica DMi8 inverted microscope with DAPI and rhodamine fluorescent filters.

References

1. J. R. Gois, N. Rocha, A. V. Popov, T. Guliashvili, K. Matyjaszewski, A. C. Serra and J. F. J. Coelho, *Polymer Chemistry* **2014**, *5*, 3919-3928.
2. J. Lad, S. Harrisson, G. Mantovani and D. M. Haddleton, *Dalton Transactions* **2003**, 4175-4180.
3. J. Du, L. Fan and Q. Liu, *Macromolecules* **2012**, *45*, 8275-8283.
4. S. Inoue, V. Frank, M. Horning, S. Kaufmann, H. Y. Yoshikawa, J. P. Madsen, A. L. Lewis, S. P. Armes and M. Tanaka, *Biomaterials Science* **2015**, *3*, 1539-1544.
5. Bastús, N. G.; Comenge, J.; Puntes, V., Kinetically Controlled Seeded Growth Synthesis of Citrate-Stabilized Gold Nanoparticles of up to 200 nm: Size Focusing versus Ostwald Ripening. *Langmuir* **2011,** 27, (17), 11098-11105.
6. Groschel, A.; Schacher, F.; Schmalz, H.; Borisov, O.; Zhulina, E.; Walther, A.; Muller, A., Precise hierarchical self-assembly of multicompartment micelles. *Nature Communications* **2012,** 3.
7. Groschel, A. H.; Walther, A.; Lobling, T. I.; Schacher, F. H.; Schmalz, H.; Muller, A. H. E., Guided hierarchical co-assembly of soft patchy nanoparticles. *Nature* **2013,** 503, (7475), 247-251.